Thermal Unfolding Used As a Probe To Characterize the Intra- and Intersubunit Stabilizing Interactions in Phosphorylating D-Glyceraldehyde-3-phosphate Dehydrogenase from *Bacillus stearothermophilus*†

Olivier Roitel,‡ Olga Ivinova,§ Vladimir Muronetz,§ Natalia Nagradova,§ and Guy Branlant*,‡

Maturation des ARN et Enzymologie Moléculaire, UMR 7567 CNRS-UHP, Université Henri Poincaré Nancy I, BP 239, 54506 Vandoeuvre-lès-Nancy Cedex, France, and A. N. Belozersky Institute of Physico-Chemical Biology, Moscow State University, Moscow 119899, Russia

Received November 21, 2001; Revised Manuscript Received February 20, 2002

ABSTRACT: Tetrameric phosphorylating glyceraldehyde-3-phosphate dehydrogenase (GAPDH) from *Bacillus stearothermophilus* can be described as a dimer of dimers with three nonequivalent interfaces. To investigate the contribution of intra- and intersubunit interactions to GAPDH thermostability, 10 residues located either at the cofactor domain (amino acids 1−148 and 313−333) or at the catalytic domain (amino acids 149−312) were mutated and the thermal unfolding of the mutants was studied by differential scanning calorimetry in the absence and presence of saturating concentrations of NAD. Disruptions of intrasubunit interactions lead to a drastic decrease in thermostability of the N313T, Y283V, and W310F mutants. Moreover, for the N313T mutant, a weakening of cooperative interactions between the catalytic and the cofactor domains and an inefficient binding of NAD are observed. This is likely the consequences of modification or loss of the hydrogen bonding network associating N313 and residues 236−238 and N313 and the nicotinamide carboxyamide of NAD, respectively. For the residues Y283 and W310, which are involved in stacking hydrophobic interactions, mutating both positions does not affect the efficiency of NAD binding. This shows that the factors involved in the thermostability of the tetrameric apo GAPDH are then different from those induced by NAD binding. Disruption of intersubunit hydrogen bonds between the catalytic domain and the NAD-binding domain of a neighboring subunit also leads to a significant destabilization of the apo tetrameric form as observed for the D282G mutant. Moreover, no efficient binding of NAD is observed. Both results are likely the consequence of a loss of hydrogen bonds across the *P*-axis and the *Q*-axis between D282 and R197 and between D282 and R52, respectively. Similar results, i.e., a destabilizing effect and inefficient NAD binding, are observed with the T34Q/T39S/L43Q mutant in which steric hindrance is introduced at the S-loop of the *R*-axis-related subunit via mutations at the adenosine subsite. The dimeric form of the D282G mutant exhibits a single partial heat absorption peak, whereas the Y46G/R52G mutant which exists only as a dimer shows two peaks. Taking into account the recent small-angle X-ray scattering studies which suggested that the dimeric form of the D282G mutant and of the dimeric Y46G/R52G mutant are of the *O*−*R* and *O*−*P* types, respectively (Vachette, unpublished results), we propose that the presence of one or two peaks in thermal unfolding of dimers is a signature of the dimer type.

Bacillus stearothermophilus (*B. stearothermophilus*) phosphorylating D-glyceraldehyde-3-phosphate dehydrogenase (GAPDH)[1] is a well-known tetrameric enzyme whose functional and structural properties have been extensively studied (*1*−*11*). High-resolution crystallographic structural studies of both apo and holo forms are available (*10*, *11*). Tetrameric phosphorylating GAPDH from *B. stearothermophilus* has been described as a "dimer of dimers" with three nonequivalent interfaces, the *P*-axis (between subunits O and P and between subunits Q and R), the *Q*-axis (between subunits O and Q and between subunits P and R) and the *R*-axis interface (between subunits O and R and between subunits P and Q). The most extensive intersubunit interactions that are formed across the *P*-axis interface have been suggested to be essential in revealing cooperativity upon NAD binding (*12*).

The polypeptide chain of each subunit is folded into two domains, the NAD-binding and the catalytic domains. The

† This research was supported by the Centre National de la Recherche Scientifique and the University Henri Poincaré Nancy I, by the Russian Foundation of Basic Research (Grant 99-04-48076) and by the Program for the Support of Scientific Schools in Russia (Grant 00-15-97758).

* To whom all correspondence should be sent. Phone no.: 33 3 83 68 43 04. Fax: 33 3 83 68 43 07. E-mail: guy.branlant@maem.uhp-nancy.fr.

‡ Université Henri Poincaré Nancy I.

§ Moscow State University.

[1] Abbreviations: GAPDH, phosphorylating D-glyceraldehyde-3-phosphate dehydrogenase; *B. stearothermophilus*, *Bacillus stearothermophilus*; *E. coli*, *Escherichia coli*; DSC, differential scanning calorimetry; G3P, D,L-glyceraldehyde-3-phosphate; 1,3-dPG, 1,3-diphosphoglyceric acid; NAD, nicotinamide adenine dinucleotide (oxidized form); NADH, nicotinamide adenine dinucleotide (reduced form); Tris, *N*-tris(hydroxymethyl)aminomethane; EDTA, ethylenediaminetetraacetic acid.

10.1021/bi012084+ CCC: $22.00
Published on Web 05/18/2002

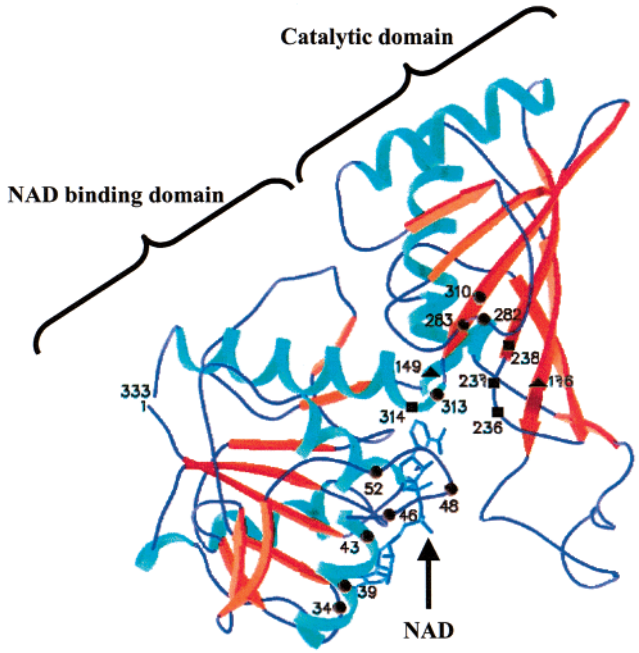

FIGURE 1: Schematic representation of the monomer *O* of the holo form of the GAPDH from *B. stearothermophilus* (*10*). The crystallographic structure was taken from the Brookhaven Protein Data Bank, access code 1gd1 (*13*). The Molscript program was used (*14*). The black circles, squares, and triangles represent the mutated residues, the hydrogen bond partners of N313 and the catalytic residues (i.e., C149 and H176), respectively. The NAD binding domain (residues 1−148 and 313−333), the catalytic domain (residues 149−312) and the NAD are also indicated.

NAD-binding domain is formed by the N-terminal half of the polypeptide chain (residues 1−148) and also includes the C-terminal α_4 helix (residues 313−330) (Figure 1). The catalytic domain is constituted by residues 149−312. On the basis of the differences observed between the apo and holo GAPDH structures from *B. stearothermophilus*, a mechanism has been proposed which accounts for conformational changes associated with NAD binding. According to this mechanism, the ADP moiety of NAD binds to GAPDH in the apo conformation. Then, domain closure within each subunit occurs, which leads to a productive binding of the nicotinamide moiety, notably, by forming a hydrogen bond between the side chain of N313 and the carboxyamide part of the pyridinium ring. In return, the rotation of the coenzyme-binding domain relative to the catalytic domain also improves interactions at the adenosine subsite. In particular, a conformational change of the main-chain residues 33−36 adjacent to D32, a residue which is essential for the adenosine positioning, is observed (*11*, *15*).

Inspection of the 3D structure shows that there exist 10 hydrogen bonds between the NAD-binding and the catalytic domains within each subunit (*15*). Moreover, a stacking hydrophobic interaction was recently characterized between Y283 located in the loop 276−289, connecting the β_5 and β_6 strands of the catalytic domain and W310 located at the end of the β_7 strand (*16*, *17*). All these intrasubunit interactions exist both in the apo and holo structures. In addition to these intrasubunit hydrogen bonds, there also exist intersubunit hydrogen bonds (*10*). A total of 26, 10, and 6 intersubunit hydrogen bonds are present along the *P*-axis, *R*-axis, and *Q*-axis interface, respectively (*10*).

The present study was done to investigate the contribution to GAPDH thermostability of different sets of hydrogen bonding, of hydrophobic interactions, or of steric hindrance between the catalytic and NAD-binding domains taking place either within a single subunit or between neighboring subunits, in the presence or absence of NAD. With this aim, different mutants, some of which are shown to exist as dimers or in dimer−tetramer equilibrium, were generated, bearing amino acid substitutions at positions involved in intra- or intersubunit stabilizing interactions. Their thermal stabilities were determined using differential scanning calorimetry (DSC). The results are presented in relation with the three-dimensional structure and the biochemical properties of GAPDH.

MATERIALS AND METHODS

Production and Purification of the Mutant GAPDHs from B. stearothermophilus. The GAPDH mutants were obtained using the site-directed mutagenesis method of Kunkel performed on a pBluescript II SK containing the *gap* gene of *B. stearothermophilus* under the control of the *lac* promoter (*18*). Wild-type and mutant GAPDHs were over-expressed and purified to homogeneity as previously described (*12*). The dimeric and tetrameric forms of mutants existing under both oligomeric states were further separated on a phenyl-Sepharose column (Pharmacia), with 200 and 600 mM ammonium sulfate, respectively. The N313T mutant and the tetrameric form of D282G and T34Q/T39S/L43Q mutants, as well as the dimeric Y46G/R48G and Y46G/R52G mutants were obtained in apo form. In contrast, the wild-type and the tetrameric form of Y283V and W310F mutants were isolated in a holo form. Their apo forms were prepared by passage through an Affi-blue gel column (Bio-Rad) (*19*). The molecular masses of all proteins were confirmed by mass spectrometry. Enzyme concentrations were determined spectrophotometrically using absorption coefficients at 280 nm of 1.17×10^5 and 1.31×10^5 M^{-1} cm^{-1} for tetrameric apo and holo enzymes, respectively (*5*, *6*). In the case of the dimeric apo enzymes, the value of 5.85×10^4 M^{-1} cm^{-1} was used.

Enzyme Assays and Kinetics. Initial rate measurements were carried out at 25 °C with a Kontron Uvikon 933 spectrophotometer by following the absorbance of NADH at 340 nm, as previously described (*12*). Data were fitted to the Michaelis−Menten equation using least-squares regression analysis to determine k_{cat} and K_M. The turnover number (k_{cat}) was expressed per active site (*N*). K_M values for NAD were determined at saturating concentrations of all other substrates. The acylation rate was determined using a SFM3 Biologic Stopped-flow apparatus by following the absorbance of NADH at 340 nm, as previously described (*6*). Briefly, the first syringe contained the enzyme (16 μN) in the buffer containing 50 mM Tris/HCl, pH 8.0, 2 mM EDTA and the second syringe contained 2 mM NAD and 2 mM D,L-glyceraldehyde-3-phosphate (G3P) in the same buffer. Data were fitted with the Biokine program using nonlinear regression analysis. An average of five runs was performed to determine each rate constant.

Absorption Band of the Binary Enzyme−NAD Complex (Racker Band). Measurements of the intensity of the absorption band centered at 360 nm (*20*) were carried out at 25 °C

as previously described (*2*). The extinction of the absorption band by 1,3-dPG (1,3-diphosphoglyceric acid; 0.5 mM final concentration for dimeric and tetrameric forms) was monitored as previously described (*21*).

Analytical Ultracentrifugation. Sedimentation of different GAPDH forms was studied using a model E Spinco analytical ultracentrifuge (Beckman), equipped with a photoelectric scanner, a multiplexer and a monochromator. A titanium rotor An-F-Ti and double-sector cells were used. The rotor speed was 261600*g*. Scanning was carried out at the wavelength 280 nm. The sedimentation velocity studies were performed at 20 °C in a buffer containing 100 mM KH_2PO_4/KOH, pH 7.5, 1 mM EDTA. The sedimentation coefficient was normalized to the standard conditions, i.e., a solvent with the density and viscosity of water at 20 °C.

Differential Scanning Calorimetry. Differential scanning calorimetry measurements were made using a DASM-4 adiabatic microcalorimeter (Biopribor, Poushchino, Russia) with a 0.47-mL cell volume at scan rates of 1.0, 0.5, and 0.125 °C/min, as previously described (*22*). All thermal transitions observed were irreversible and scan-rate dependent. Both for the wild type and different mutants, decreasing scanning rate from 1 to 0.125 °C/min resulted in a shift of T_{max} (maximum of the thermal transition peak) by 2.5−3 °C toward lower temperatures, with no changes in the shape of the curves. Therefore, all experiments throughout this study were performed at a constant scan-rate of 1 °C/min. Instrumental baselines recorded when both cells were filled with buffer were subtracted from experimental traces to obtain the heat capacity curves. The values of T_{max} and calorimetric enthalpies (ΔH_{cal}) were determined using original software. Due to the irreversibility of the heat denaturation process, it was impossible to calculate the value of the van't Hoff enthalpy, and this precluded its comparison with the calorimetrically determined enthalpy and the determination of the ratio $\Delta H_{cal}/\Delta H^{van't\ Hoff}$, the parameter widely used to estimate the degree of cooperativity of unfolding transitions (*23*). Therefore, the unfolding transition curves were only compared in terms of the width of the corresponding peaks (measured at half-height).

RESULTS

Justification of the Mutations. A total of 10 residues involved in the interactions between the cofactor domain (residues 1−148 and 313−333) and the catalytic domain (residues 149−312) or within the catalytic domain were mutated. Residues N313, Y283, and W310 are involved in intrasubunit interactions, whereas residues Y46, S48, R52, and D282 are involved in intersubunit interactions. Residues T34, T39, and L43 are located close to the sites of intersubunit interactions.

N313, which is located in the α_4 helix of the NAD-binding domain (Figure 1), forms a network of hydrogen bonds, including: (i) three hydrogen bonds with residues 236−238 positioned in the β_4 strand (residues 238−246), and the nearby loop (residues 234−237) of the catalytic domain from the same subunit (Table 1); (ii) one hydrogen bond through water with neighboring E314; (iii) one hydrogen bond with the oxygen atom of the carboxyamide group of NAD; and (iv) one hydrogen bond with NAD atom 07N (*10*, *15*). N313 was replaced by threonine.

Table 1: Hydrogen Bonds between Residues of the NAD-binding and the Catalytic Domains of GAPDH from *B. Stearothermophilus* (*15*)

NAD binding domain		catalytic domain	
V49	O	N284	ND2
N146	O	N152	ND2
D312	OD1	N236	ND2
D312	OD2	G285	N
N313	OD1	V237	N
N313	OD1	S238	OG
N313	ND2	N236	OD1
G316	N	S286	O
*R*320	NZ	G269	O
*R*320	NZ	T287	O

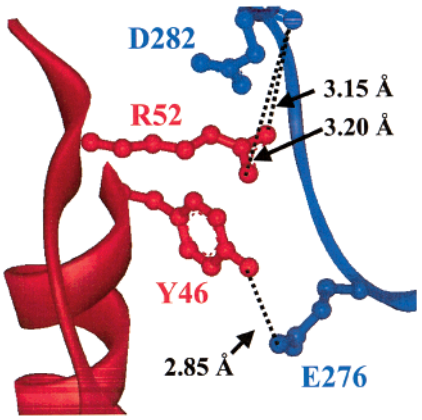

FIGURE 2: Intersubunit hydrogen bonds formed between residues R52−D282 and Y46−E276 across the *Q*-axis interface of the GAPDH from *B. stearothermophilus*. The crystallographic structure of the holo GAPDH from *B. stearothermophilus* was taken from the Brookhaven Protein Data Bank, access code 1gd1 (*13*). The WebLabViewerPro program version 3.7 (Molecular Simulations, Inc.) was used. The monomer *O* and *Q* are represented in red and blue, respectively. Dashed lines represent the hydrogen bonds formed between the side chains of Y46 and E276 and between the side chain of R52 and the C═O of the main chain of D282. The length of each hydrogen bond is also indicated.

Y283 and W310 are located in the loop following the strand β_5 (residues 276−289) and in the strand β_7 in the catalytic domain, respectively (Figure 1). Y283 and W310 form an intramonomeric stacking interaction and were replaced by valine and phenylalanine, respectively (*17*).

T39 and L43 are located in the helix α_c, whereas T34 is located in the preceding loop within the cofactor domain (Figure 1). T34, T39, and L43 were replaced with glutamine, serine, and glutamine, respectively. The triple mutation was introduced in the region where the adenosine phosphate portion of NAD binds, namely, close to D32, which is essential for the efficient binding of the coenzyme. The selected residues, which are not involved in hydrogen bonds, neither with NAD nor with any amino acid residue, border a cavity filled by the S-loop of the *R*-axis-related subunit. The mutations were designed to form a hydrogen bond network which should fill this cavity.

Y46, S48, and R52 are located in the loop following the helix α_c in the cofactor domain (Figure 1) and form hydrogen bonds with residues of the catalytic domain of another subunit. Y46−E276 and R52−D282 are the hydrogen bond partners across the *Q*-axis interface (Figure 2), whereas S48 and both D186 and R197 are hydrogen bond partners across the *R*-axis interface (Figure 3). D282, which is located in

Table 2: Biochemical Properties of GAPDH Mutants

mutation	kinetic parameters[a]			$\epsilon_{360\ nm,\ monomer}$ of the binary enzyme NAD complex[b]	
	k_{cat} (s^{-1})	K_M NAD (mM)	acylation rate (s^{-1})	($M^{-1}\ cm^{-1}$)	$S_{W,20}$ (S)
wild type (T)	65 ± 7	0.05 ± 0.01	320 ± 60	1000 ± 75	6.49 ± 0.39
Y283V (T)	73 ± 9	0.06 ± 0.01	300 ± 45	890 ± 35	6.53 ± 0.30
W310F (T)	51 ± 6	0.10 ± 0.02	310 ± 62	920 ± 50	6.28 ± 0.45
N313T (T)	1.0 ± 0.2	2.5 ± 0.3	0.8 ± 0.1	180 ± 40	6.30 ± 0.35
T34Q/T39S/L43Q (T)	0.10 ± 0.02	0.29 ± 0.03	305 ± 60	250 ± 30	7.07 ± 0.12
D282G (T)	0.10 ± 0.02	0.20 ± 0.03	290 ± 44	200 ± 42	6.57 ± 0.12
Y283V (D)	nda			87 ± 22	4.29 ± 0.32
D282G (D)	nda			75 ± 15	ND[c]
T34Q/T39S/L43Q (D)	nda			122 ± 20	4.30 ± 0.22
Y46G/S48G (D)	nda			90 ± 11	3.99 ± 0.21
Y46G/R52G (D)	nda			110 ± 17	ND

[a] The k_{cat} and K_M values were determined at saturating concentrations of all other substrates and expressed in terms of monomer. No detectable activity (nda) means activity $<10^{-3}\ s^{-1}$. [b] Differential spectroscopic measurements were carried out at 25 °C with two matched double-compartment cells. Enzyme concentrations were 80 μM in subunits for both tetrameric and dimeric GAPDHs. [c] ND: not determined, (T) and (D) designate the tetramer and dimer, respectively.

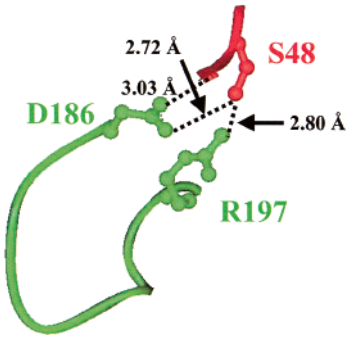

FIGURE 3: Intersubunit hydrogen bonds formed between residues S48 and both D186 and R197 across the *R*-axis interface of the GAPDH from *B. stearothermophilus*. The monomers *O* and *R* are represented in red and green, respectively. Dashed lines represent the hydrogen bonds formed between the side chains of S48 and both D186 and R197 and between the side chain of D186 and the NH group of the main chain of S48. The length of each hydrogen bond is also indicated.

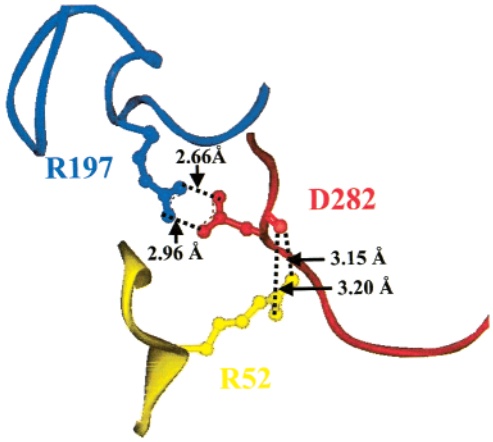

FIGURE 4: Intersubunit hydrogen bonds formed between residues D282 and both R52 and R197 across the *P*-axis and *Q*-axis interfaces of the GAPDH from *B. stearothermophilus*, respectively. The monomers *O*, *P*, and *Q* are represented in red, blue and yellow, respectively. Dashed lines represent the hydrogen bonds formed between the side chain of R52 and the C=O of the main chain of D282 and between the side chains of R197 and D282. The length of each hydrogen bond is also indicated.

the loop following the strand β_5 (residues 276−289) in the catalytic domain, forms hydrogen bonds with R197 and R52 across the *P* and *Q*-axis interfaces, respectively (Figure 4). Y46, S48, R52, and D282 were replaced with glycine, which was expected to minimize conformational alterations of the loops.

Biochemical Properties of GAPDH Mutants. The W310F and N313T mutants only existed as tetramers, whereas the T34Q/T39S/L43Q, D282G, and Y283V mutants were shown to exist as both tetramers and dimers. Both oligomeric forms were easily separated on phenyl-Sepharose. The fact that the rate of the dimer-tetramer equilibrium was shown to be very slow (Roitel, unpublished results) excluded any significant interconversion of the two forms during the duration of the various experiments. The double Y46G/R52G mutant only existed as dimers, a result similar to that already obtained for the double Y46G/S48G mutant (*12*). In all cases, the dimeric and tetrameric states were confirmed by the determination of the Svedberg coefficients (Table 2).

Under full saturation with NAD, the tetrameric forms of the Y283V and W310F mutants exhibited an absorption band centered at 360 nm called the Racker band whose intensity was similar to that of the wild-type enzyme. The tetrameric N313T mutant and the tetrameric forms of T34Q/T39S/L43Q and D282G mutants exhibited a 4−5-fold lower intensity whereas all dimeric mutants exhibited a 8−13-fold lower intensity (Table 2). As already shown (*2*), the Racker band is a consequence of the formation of a charge-transfer transition between the thiolate of C149 and the pyridinium ring, acting as an electron donor and electron acceptor, respectively. The fact that addition of 1,3-dPG to all tetrameric and dimeric mutants and the wild-type enzyme led to a total disappearance of the absorption band reinforces this interpretation (curves not shown).

All tetrameric forms were enzymatically active. However, whereas the k_{cat} values of the tetrameric Y283V and W310F mutants were similar to those of the wild-type enzyme, the N313 substitution with a threonine resulted in a 65-fold decrease in the k_{cat} with a 50-fold increase in the K_M for NAD. The K_D value determined for NAD is 50 μM that is 50-fold lower than the K_M value (*24*). The k_{cat} values of both the tetrameric forms of T34Q/T39S/L43Q and D282G mutants were more drastically decreased by a factor of 650, while K_M values for NAD were only increased by a factor of 4. For all mutants except N313T, the acylation rate was similar to that of the wild type (Table 2).

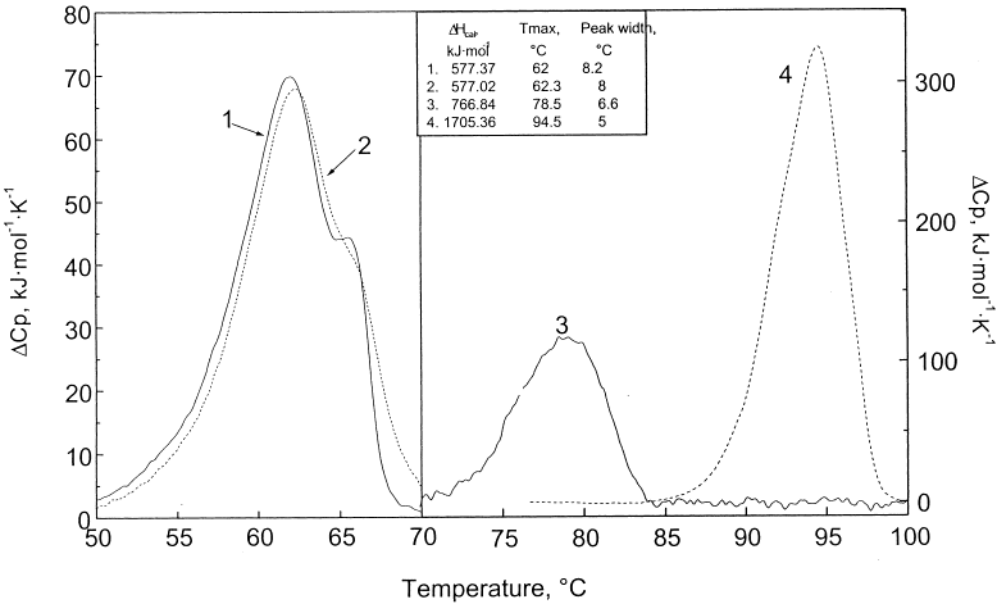

FIGURE 5: The temperature dependence of the partial heat capacity of the apo tetrameric forms of the N313T mutant and of the wild-type enzyme in the absence (curves 1 and 3, respectively) and the presence of 2.5 mM NAD (curves 2 and 4, respectively). The protein concentration is 1 mg/mL. Buffer: 100 mM KH_2PO_4/KOH, pH 7.5, 1 mM EDTA.

Table 3: Thermal Unfolding of the Tetrameric and Dimeric Mutant GAPDHs

	apo enzyme	+2.5 mM NAD
mutation	T_{max} (°C)	T_{max} (°C)
wild type (T)[a]	78.5 ± 0.4	94.5 ± 0.3
N313T (T)	62.0 ± 0.5/65.5 ± 0.5	62.3 ± 0.5
W310F (T)	70.7 ± 0.4	88.5 ± 0.4
Y283V (T)	68.4 ± 0.5	88.2 ± 0.4
D282G (T)	70.3 ± 0.5	71.4 ± 0.5
T34Q/T39S/L43Q (T)	64.8 ± 0.3	66.8 ± 0.3
Y283V (D)	73.5 ± 0.5	74.5 ± 0.5
D282G (D)	71 ± 0.4	71.6 ± 0.4
T34Q/T39S/L43Q (D)	64.8 ± 0.5/70.2 ± 0.5	ND[b]
Y46G/S48G (D)	65.4 ± 0.5/70.2 ± 0.5	66.2 ± 0.5/71.2 ± 0.5
Y46G/R52G (D)	65.5 ± 0.5/70.2 ± 0.5	66.2 ± 0.5/70.9 ± 0.5

[a] (T) and (D) designate the tetramer and dimer, respectively. [b] ND: not determined.

All dimeric mutants were shown to be inactive similarly to that previously described for double Y46G/S48G mutant (Table 2) (*12*). The free NAD concentrations at half-saturation which is indicative of NAD affinity were also determined for all dimeric mutants and were shown to be similar or lower than the value of 2.8 μM previously determined for the Y46G/S48G mutant (Roitel, unpublished results, *12*).

Thermal Unfolding Properties of GAPDHs Mutated at Sites Involved in Intrasubunit Interactions. Figure 5 shows the partial heat capacity curves obtained with the N313T mutant in the absence and the presence of saturating concentrations of NAD, in comparison with the wild-type enzyme. The partial heat capacity profile of the N313T mutant broadened and two maxima appeared at 62.0 and 65.5 °C. NAD binding was unable to increase significantly the thermostability of the mutant (Table 3).

Figures 6 and 7 show the thermograms obtained with the apo tetrameric W310F and Y283V mutants in the absence and in the presence of NAD. The replacement of W310 and Y283 with phenylalanine and valine, respectively, markedly reduced the T_{max} values of the apo mutants by 7.8 and 10 °C, respectively, as compared to that of the wild-type apo enzyme. The effect of NAD binding was highly pronounced with an increase of T_{max} by 17.8, 19.8, and 16 °C for the W310F, Y283V mutants and wild type, respectively (Table 3). As for the wild type, the thermal transitions of both W310F and Y283V mutants appeared to be symmetrical.

Thermal Unfolding Properties of GAPDHs Mutated at Sites Involved in Intersubunit Interactions. Mutating D282 into glycine resulted in a destabilization of the apo tetrameric form of the mutant with a T_{max} decrease of 8.2 °C and in an asymmetry of the thermal transition. The addition of saturating concentrations of NAD did not significantly affect the thermal unfolding characteristics (Figure 8, Table 3).

The tetrameric apo form of the T34Q/T39S/L43Q mutant showed a strongly reduced thermostability with a shift of the T_{max} by 14 °C and an asymmetric thermal transition compared to the wild-type apo enzyme. Again, as observed for the D282G mutant, only a slight effect upon addition of a saturating concentration of NAD was observed (Figure 9, Table 3).

Both apo dimeric forms of the D282G and Y283V mutants exhibited a single sharpened asymmetric heat absorption peak with T_{max} values at 71 and 73.5 °C, respectively, whereas the apo dimeric form of the T34Q/T39S/L43Q mutant (Table 3), and the dimeric Y46G/S48G and Y46G/R52G mutants showed two well-separated peak maxima at around 65 and 70 °C, respectively (Figure 10). In all cases, the binding of NAD did not significantly change the thermal characteristics of the dimeric forms (Table 3, Figures 7−10).

DISCUSSION

The aim of the present study was to determine: (i) the contribution of intrasubunit and intersubunit interactions between the cofactor domain and the catalytic domain or interactions within the catalytic domain itself, to the thermostability of apo GAPDH from *B. stearothermophilus*; and (ii) whether the efficiency of NAD binding depends on these stabilizing interactions. To investigate these points, different

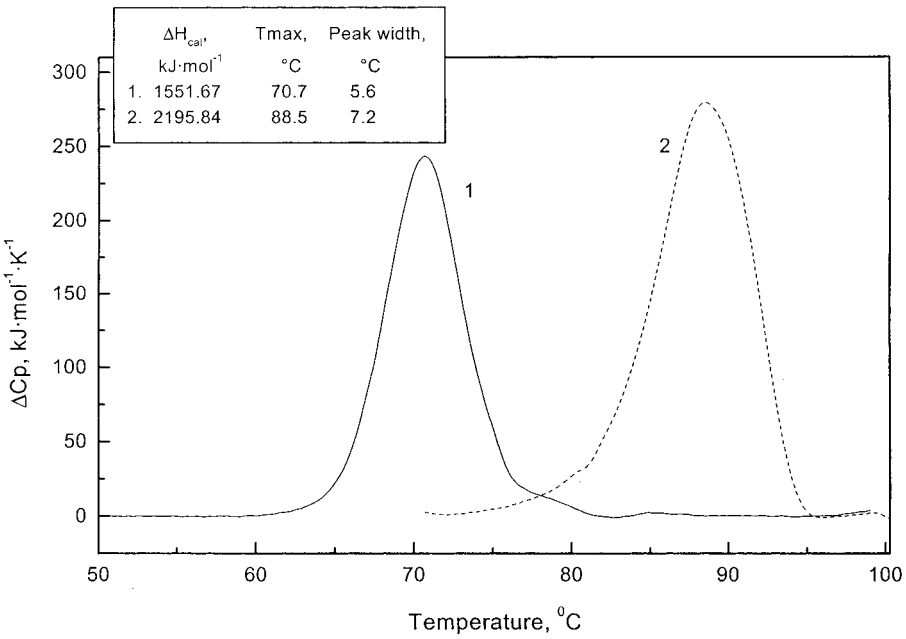

FIGURE 6: The temperature dependence of the partial heat capacity of the apo tetrameric form of the W310F mutant in the absence (curve 1) and the presence of 3 mM NAD (curve 2). Other conditions are the same as in Figure 5.

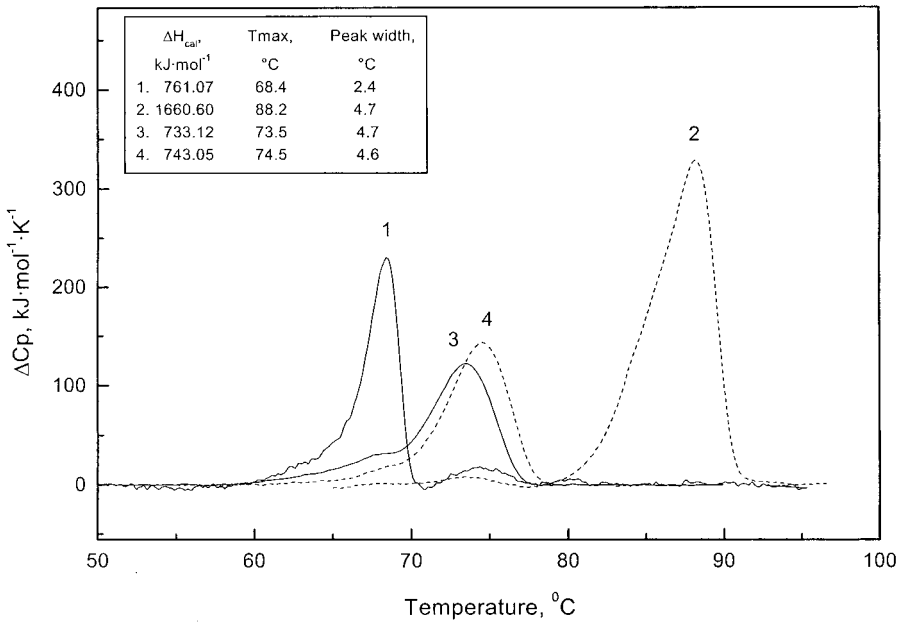

FIGURE 7: The temperature dependence of the partial heat capacity of the apo tetrameric and dimeric forms of Y283V mutant in the absence (curves 1 and 3, respectively) and the presence of 2.5 mM NAD (curves 2 and 4, respectively). The protein concentrations are 0.1 and 0.5 mg/mL for tetrameric and dimeric forms, respectively. Other conditions are the same as in Figure 5.

mutations were introduced either at the catalytic or cofactor domains, and also at the subunit interfaces in order to compare in the latter case the stability of dimers relative to their tetrameric counterparts.

The Role of Intrasubunit Interactions in the Stabilization of apo and holo GAPDH Structure. Substituting threonine for N313 resulted in a drastic decrease of the stability and in the broadening of the partial heat capacity curve of the N313T mutant. The appearance of two peaks on the melting curve indicates that the thermal unfolding transition is becoming less cooperative. The T_{max} of the less stable peak, i.e., 62 °C, coincides with the T_{max} of the separated NAD-binding domain of *B. stearothermophilus* GAPDH (*22*). This suggests that the first peak corresponds to the NAD-binding domain. The mutation of asparagine into threonine likely disrupts the hydrogen bonding network formed between the side chains of N313 and (i) of residues 236 to 238 as shown in the case of the *Escherichia coli* N313T mutant (*15*); and (ii) of the neighboring residue E314 (through a water molecule) (*10*). Taken together, this would lead to a significant weakening of the interdomain interactions within each subunit and can therefore explain the strong decrease of the T_{max}.

Binding of NAD had no significant effect on the thermal unfolding properties of the apo form of the N313T mutant. This suggests that the mutation precluded an efficient binding of NAD. Such a conclusion is supported by the intensity of the absorption band at 360 nm, which is a probe of the

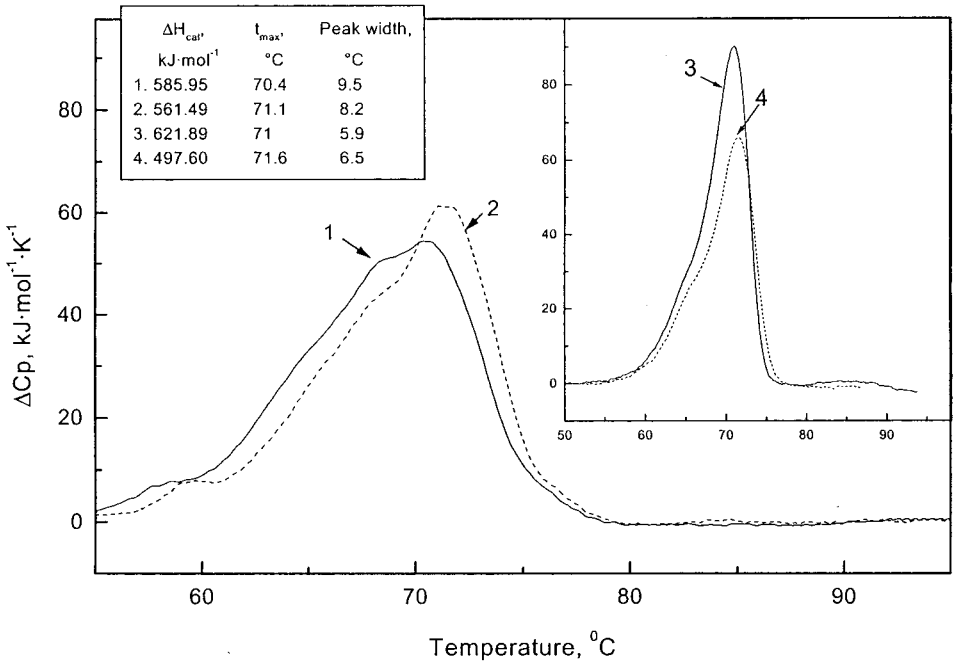

FIGURE 8: The temperature dependence of the partial heat capacity of the apo tetrameric form of the D282G mutant in the absence (curve 1) and the presence of 2.5 mM NAD (curve 2). Inset: the thermograms of the apo dimeric form of the D282G mutant in the absence (curve 3) and the presence of 2.5 mM NAD (curve 4). The protein concentration is 1 mg/mL. Other conditions are the same as in Figure 5.

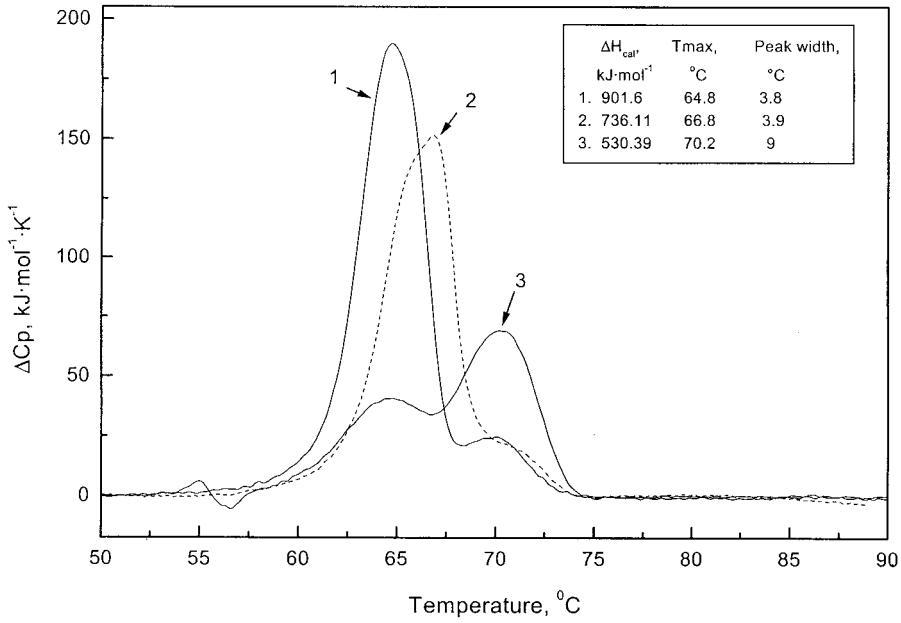

FIGURE 9: The temperature dependence of the partial heat capacity of the apo tetrameric form of the T34Q/T39S/L43Q mutant in the absence (curve 1) and the presence of 2.5 mM NAD (curve 2) and of the its apo dimeric form in the absence of NAD (curve 3). The protein concentration is 0.6 mg/mL. Other conditions are the same as in Figure 5.

relative positioning of C149 and of the pyridinium ring of NAD, which is 5-fold less than that exhibited by the wild type. This is also supported by the 400-fold decrease in acylation rate and the 50-fold increase of K_D value for NAD (*24*). All these results are in agreement with the high-resolution structural study carried out on the N313T mutant GAPDH from *Escherichia coli* which showed a structure of the *E. coli* N313T mutant saturated with NAD rather more similar to the apo than to the holo conformation (*15*). Although no significant effect was observed upon NAD binding, the thermogram seems to be composed of only one transition in contrast to the apo form for which two transitions were observed. Therefore, this suggests that the catalytic and cofactor domains interact more strongly in the presence of NAD.

Mutating Y283 into valine and W310 into phenylalanine markedly decreased the thermostability of both mutants by at least 6 °C for the apo and the holo forms as well. Both mutants exhibited a symmetrical nondissociating thermal transition for the apo and the holo forms as well (Table 3, Figures 6 and 7). However, neither mutation significantly affected the efficiency of NAD binding as evidenced by the isolation of both mutants as holo enzymes and by the Racker band intensity and specific activities which are similar to

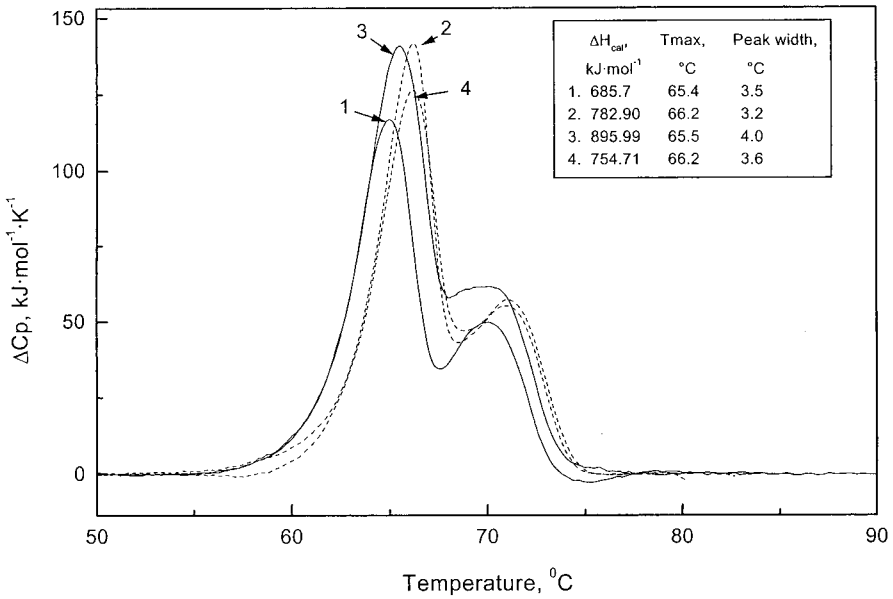

FIGURE 10: The temperature dependence of the partial heat capacity of the dimers of the Y46G/S48G and Y46G/R52G mutants in the absence (curves 1 and 3, respectively) and the presence of 2.5 mM NAD (curves 2 and 4, respectively). The protein concentration is 1 mg/mL. Other conditions are the same as in Figure 5.

those of the wild-type enzyme. Therefore, efficient binding of NAD and subsequent conformational changes necessary for formation of a competent active center are operative. Moreover, in the presence of a saturating NAD concentration, the T_{max} values of both mutants were increased by 17 to 20 °C similar to what is observed with the wild type. Therefore, it can be concluded that (i) the stacking hydrophobic interaction between Y283 and W310 is essential for stabilizing both the apo and the holo tetrameric forms; and (ii) the effect of NAD binding on the thermostability of GAPDH does not depend on the Y283−W310 interaction. Consequently, this strongly suggests that the factors involved in the thermostability of the tetrameric apo GAPDH are different from those induced by the NAD binding.

The Role of Intersubunit Domain Interactions in the Stabilization of apo and holo GAPDH. The rupture of hydrogen bonding interactions between the catalytic and NAD-binding domains belonging to neighboring subunits also led to a strong destabilization of the tetrameric GAPDH and to a weaker interaction between the cofactor and the catalytic domains. This is well illustrated by the results obtained on the D282G and the T34Q/T39S/L43Q mutants. In the case of the apo tetrameric form of the D282G mutant, a 8 °C decrease in T_{max} and an increase in the peak width were observed. This is likely due to the disruption of hydrogen bonds between position 282 and (i) R197 across the *P*-axis interface; and (ii) R52 across the *Q*-axis interface. Rupture of these interactions is expected to prevent an efficient NAD binding. This is confirmed by the fact that (i) the tetrameric form of the D282G mutant was isolated as an apo form; (ii) the intensity of the Racker band was 5-fold lower than that for the wild-type enzyme; and (iii) no significant increase in the thermostability was observed in the presence of a saturating concentration of NAD. In the case of the triple T34Q/T39S/L43Q mutant, the destabilizing effect was even more pronounced with a 14 °C decrease in T_{max}. No significant stabilizing effect of NAD binding was observed. Again, the intensity of the Racker band was 5-fold smaller suggesting an inefficient binding of the nicotinamide moiety. This improper binding is probably the consequence of an inefficient binding of the adenosine moiety due to the mutation of T34 located in the adenosine subsite and which in return should perturb the nicotinamide binding.

Properties of Mutant Dimers. The dimeric forms of the D282G and Y46G/R52G mutants showed significant differences in their thermal unfolding characteristics. Whereas the D282G mutant exhibited a single partial heat absorption peak with a T_{max} at 71 °C, the dimeric Y46G/R52G mutant displayed two peaks with T_{max} values at around 65 and 70 °C, respectively. Recently, the results obtained in small-angle X-ray scattering studies have suggested that the dimeric D282G and Y46G/R52G mutants are of the *O*−*R* and the *O*−*P* type, respectively (Vachette, unpublished data). Therefore, it is tempting to hypothesize that the presence of one or two peaks in thermal unfolding of dimers is a signature of the *O*−*R* and *O*−*P* dimers, respectively. Then, on the basis of their thermal unfolding profiles, we propose that the dimeric form of the Y283V mutant is of the *O*−*R* type whereas the dimeric Y46G/S48G mutant and the dimeric form of the T34Q/T39S/L43Q mutant are of the *O*−*P* type. X-ray scattering studies are in progress to validate these hypotheses. In this context, it remains to elucidate at the structural level the reasons behind the different thermal behaviors of the *O*−*P* and *O*−*R* dimers.

The Y283V and T34Q/T39S/L43Q mutants were shown to exist in a slow dimer−tetramer equilibrium (Roitel, unpublished data). In the case of the Y283V mutant, the mutation is located next to D282. Thus, the dissociation of the tetrameric form of the Y283V mutant is likely due to the disruption of stabilizing interactions formed by neighboring residues in the 276−289 loop, i.e., R281 and D282, across the *P*-axis interface as for the D282G mutant and not to loss of the hydrophobic interaction with W310. Indeed, the W310F mutant remained tetrameric. For the triple T34Q/T39S/L43Q mutant, the dissociation of the tetramers into dimers is likely due to the steric hindrance at the *R*-axis interface, because these mutations formed a hydrogen bond

network which fills the cavity occupied by the S-loop of the *R*-axis-related subunit.

The binding of NAD produced no significant thermal stabilization of any dimers, as also illustrated by the low intensities of the Racker band in all dimers. The fact that even in the presence of the substrate neither the acylation step nor the phosphorylation is catalytically efficient shows that introducing mutations at both the *P*- and *Q*-axis interfaces provokes significant conformational rearrangements which prevent the formation of not only a holo dimeric form but also a competent ternary complex. Knowledge of the X-ray structure for both types of dimers would be informative.

Finally, our study shows that the dimeric apo forms of mutants, which exist in both tetrameric and dimeric forms, are at least as stable as the parent tetramers. The thermostability of the dimeric form of the Y283V mutant is even significantly higher than that of its tetrameric form. This is unusual since, generally, dissociated oligomeric enzymes are less stable than their nondissociated counterparts (*25*).

ACKNOWLEDGMENT

We thank V. Orlov and V. Michurina for their help in DSC experiments. We are very grateful to S. Sanglier, Dr. H. Rogniaux and Dr. A. Van Dorsselaer for determining the molecular masses of wild type and mutant GAPDHs and to Dr. E. Duée for helpful discussions.

REFERENCES

1. Harris, J. I., and Waters, M. (1976) in *The Enzymes* (Boyer, P. D., Ed) Vol. 13, pp 1−49, Academic Press, New York.
2. Mougin, A., Corbier, C., Soukri, A., Wonacott, A., Branlant, C., and Branlant, G. (1988) *Protein Eng. 2*, 45−48.
3. Branlant, C., Oster, T., and Branlant, G. (1989) *Gene 75*, 145−155.
4. Corbier, C., Branlant, C., Wonacott, A., and Branlant, G. (1989) *Protein Eng. 2*, 559−562.
5. Corbier, C., Clermont, S., Billard, P., Skarzynski, T., Branlant, C., Wonacott, A., and Branlant, G. (1990) *Biochemistry 29*, 7101−7106.
6. Corbier, C., Mougin, A., Mely, Y., Adolph, H. W., Zeppezauer, M., Gerard, D., Wonacott, A., and Branlant, G. (1990) *Biochimie 72*, 545−554.
7. Clermont, S., Corbier, C., Mely, Y., Gerard, D., Wonacott, A., and Branlant, G. (1993) *Biochemistry 32*, 10178−10184.
8. Corbier, C., Michels, S., Wonacott, A. J., and Branlant, G. (1994) *Biochemistry 33*, 3260−3265.
9. Michels, S., Rogalska, E., and Branlant, G. (1996) *Eur. J. Biochem. 235*, 641−647.
10. Skarzynski, T., Moody, P. C., and Wonacott, A. J. (1987) *J. Mol. Biol. 193*, 171−187.
11. Skarzynski, T., and Wonacott, A. J. (1988) *J. Mol. Biol. 203*, 1097−1118.
12. Roitel, O., Sergienko, E., and Branlant, G. (1999) *Biochemistry 38*, 16084−16091.
13. Bernstein, F. C., Koetzle, T. F., William, G. J. B., Meyer, E. F., Brice, M. D., Rodgers, J. R., Kennard, O., Shimanouchi, T., and Tasumi, M. (1977) *J. Mol. Biol. 112*, 535−542.
14. Kraulis, P. J. (1991) *J. Applied Crystallogr. 24*, 946−950.
15. Duée, E., Olivier-Deyris, L., Fanchon, E., Corbier, C., Branlant, G., and Dideberg, O. (1996) *J. Mol. Biol. 257*, 814−838.
16. Gabellieri, E., Rahuel-Clermont, S., Branlant, G., and Strambini, G. B. (1996) *Biochemistry 35*, 12549−12559.
17. Strambini, G. B., Gabellieri, E., Gonnelli, M., Rahuel-Clermont, S., and Branlant, G. (1988) *Biophys. J. 74*, 3165−3172.
18. Kunkel, T. A., Bebenek, K., and McClary, J. (1991) *Methods Enzymol. 204*, 125−139.
19. Talfournier, F., Colloc′h, N., Mornon, J. P., and Branlant, G. (1998) *Eur. J. Biochem. 252*, 447−457.
20. Racker, E., and Krimsky, I. (1952) *J. Biol. Chem. 198*, 741−743.
21. Harrigan, P. J., and Trentham, D. R. (1973) *Biochem. J. 135*, 695−703.
22. Levashov, P., Orlov, V., Boschi-Muller, S., Talfournier, F., Asryants, R., Bulatnikov, I., Muronetz, V., Branlant, G., and Nagradova, N. K. (1999) *Biochim. Biophys. Acta 1433*, 294−306.
23. Jaenicke, R. (1991) *Eur. J. Biochem. 202*, 715−728.
24. Eyschen, J. (1997) Ph.D. Thesis, University Henri Poincaré Nancy I.
25. Neet, K. E., and Timm, D. E. (1994) *Protein Sci. 3*, 2167−2174.

BI012084+